Regular Article

ANALYTICAL
AND BIOANALYTICAL
CHEMISTRY
RESEARCH

Published by the
Iranian Chemical Society

***Anal. Bioanal. Chem. Res.**, Vol. 10, No. 4, 435-443, September 2023.*

MIP/GO/GCE Sensor for the Determination of Aminophylline in Pharmaceutical Ingredients and Urine Samples

Aya Saher[a], A. B. Abdallah[a], Ahmed Fathi Salem Molouk[a], Wael I. Mortada[b,*] and Magdi E. Khalifa[a]

[a]*Department of Chemistry, Faculty of Science, Mansoura University, Mansoura 35516, Egypt*

[b]*Urology and Nephrology Center, Mansoura University, Mansoura 35516, Egypt*

(Received 9 April 2023, Accepted 3 June 2023)

A new selective molecular imprinted polymer (MIP) was synthesized for the electrochemical sensing of aminophylline (AMI). The MIP was fabricated *via* the co-polymerization of different monomers (acrylamide and methacrylic acid) around the template (AMI) in the presence of a cross-linker (ethylene glycol dimethacrylate) and an initiator (potassium persulfate). The prepared polymers were characterized by CHN elemental analysis, Fourier-transform infrared spectroscopy, atomic force microscopy, and scanning electron microscopy. For electrochemical applications, a voltammetric sensor was constructed by dropping MIP on the glassy carbon electrode surface after modification with the graphene oxide. Electrochemical determinations were achieved using differential pulse voltammetry (DPV), which indicated a wide range (3.7×10^{-11}-1×10^{-3} M) of AMI and a low detection limit (2.1×10^{-12} M). Alternatively, MIP was immobilized on a plasticized PVC membrane and deposited as one layer on the GCE to fabricate the potentiometric sensor. In the same context, a potentiometric sensor was constructed and exhibited a linear calibration curve in the concentration range of 2.6×10^{-9} M to 3.1×10^{-3} M, with a detection limit of 1.5×10^{-10} M. Additionally, the developed methods displayed great selectivity for AMI compared to other competing molecules, high repeatability, and stability. In addition, the proposed methods were successfully applied for AMI detection in pharmaceutical drugs with recovery values (98.2-99.6%).

Keywords: Aminophylline, Bronchodilator drug, Molecularly imprinted polymer, Electrochemical sensors

INTRODUCTION

Aminophylline (AMI) is a therapeutic drug consisting of a combination of theophylline and ethylenediamine (Fig. 1). Ethylenediamine makes theophylline more water-soluble. It is most commonly utilized for bronchial asthma and has been investigated for several medical applications. Aminophylline belongs to a group of medicines known as bronchodilators. Bronchodilators relax the muscles in the bronchial tubes (air passages) of the lungs. They relieve cough, wheezing, shortness of breath, and troubled breathing by increasing the airflow through bronchial tubes. It is also used in the treatment of certain respiratory disorders such as chronic bronchitis, emphysema, and chronic obstructive pulmonary diseases [1-3]. The spread of coronavirus at the latest times has made the use of AMI medicine return to the spot. Coronaviruses affect people of all ages, genders, and various health statuses. People with chronic diseases or other health conditions may have a severe illness from COVID-19. There are no specific drugs targeting the coronavirus. Aminophylline is a phosphodiesterase enzyme inhibitor that stimulates the respiratory center and peripherally relaxes bronchial smooth muscle, which explains its anti-hypoxic effect. A study aimed to show the effect of AMI as an anti-hypoxic agent as an add-on therapy to the high flow rate of oxygen in COVID-19 patients who presented with low blood oxygen. Aminophylline therapy is effective in relieving hypoxia by elevating blood saturation with oxygen to 100%

*Corresponding author. E-mail: w.mortada@mans.edu.eg

(10 out of 10 patients) in COVID-19 patients without evidence of risk factors or concomitant diseases. The effectiveness of AMI declined to 81.9% in patients with concomitant diseases, and it was ineffective in four patients, three of whom survived with artificial ventilation and one of whom died despite using all supportive measures. In conclusion, AMI as an anti-hypoxic agent was associated with improved outcomes in severe COVID-19. Its effect extends to patients with risk factors or concomitant diseases [4,5]. Owing to the narrow therapeutic window of AMI and its possible adverse side effects, the concentration of AMI should be monitored, especially after starting therapy [6].

Numerous analytical techniques, including high-performance liquid chromatography (HPLC) [7], liquid chromatography-tandem mass spectrometry (LC-TMS) [8], capillary electrophoresis (CE) [9], Raman spectroscopy [10], spectrophotometry [11], fluorescence sensors [12], and chemiluminescence [13] are commonly used to assess the amount of AMI.

Although these methods are the most utilized in the routine analysis of AMI in various samples, they have various disadvantages, such as the pretreatment of the sample being of significant experiments, the instruments being intricate, and their long detection time. Electrochemical methods are robust analytical methods that possess numerous advantages such as simplicity, low instrument cost, long linear range, and excellent stability [14-16]. The incorporation of molecularly imprinted polymers (MIPs) with sensor technology has considerable potential for the development of devices that offer significant merits, including *in-situ* preparation, high sensitivity, and acceptable accuracy and precision, compared to current methodologies [17-23].

Molecularly imprinted polymers are artificial synthetic receptors with complementary cavities matching the size and shape of the target analyte [24]. A specific recognition system for MIP was created by covalent and/or non-covalent bonds between the template and functional monomers. Consequently, a crosslinker is polymerized around the template-monomer complex in the presence of an initiator. Subsequently, the template molecules are eluted from the polymeric matrices, leaving imprinting sites for template molecules [25]. Owing to the superb selectivity and high robustness of the synthesized polymers, they have been

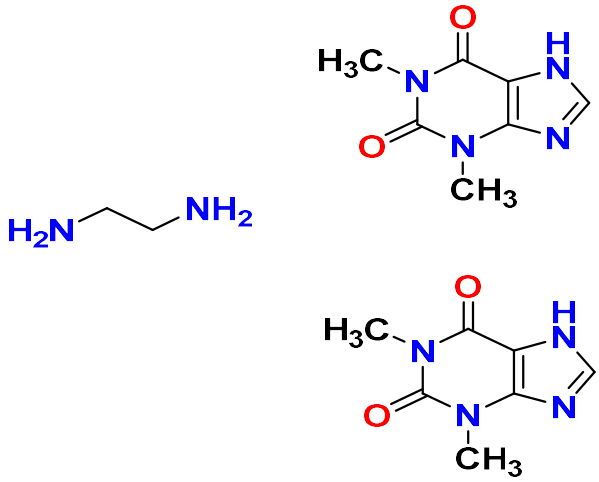

Fig. 1. The chemical structure of aminophylline.

widely used in various applications, including biomarker protein recognition [26], enantiomeric separation, food safety, drug delivery, solid-phase extraction (SPE), and sensors [27-30].

In this study, MIPs were synthesized for preconcentration and electrochemical sensing of AMI in real samples. Notably, this is the first trial to use MIP for selective detection and monitoring of AMI using different electrochemical techniques. The imprinted polymer was first synthesized and then dropped onto the surface of a glassy carbon electrode (GCE) after modification with graphene oxide to fabricate an electrochemical voltammetric sensor. The prepared polymers were characterized by various techniques. For comparison, an imprinted potentiometric sensor was constructed by immobilizing the prepared polymer in a plasticized polyvinyl chloride (PVC) membrane and depositing it on the GCE as one layer. After optimizing the analytical parameters, the proposed techniques were applied for the selective detection of AMI in pharmaceutical drugs and urine samples.

EXPERIMENTAL

Chemicals and Solutions

Double-distilled water was used for the preparation of all aqueous solutions, and all chemicals that were used in the current investigation were of analytical reagent grade and used as received. Highly pure AMI powder was obtained from Alfa Aesar (Karlsruhe, Germany). Di-butyl phosphate

(DBP), dioctyl sebacate (DOS), and tri-cresyl phosphate (TCP) were purchased from Fluka (Buchs, Switzerland). Methacrylic acid (MAA), acrylamide (AM), PVC, potassium persulfate, potassium chloride (KCl), ethylene glycol dimethyl acrylate (EGDMA), o-nitrophenyl octyl ether (o-NPOE), dioctyl phthalate (DOP), potassium ferricyanide ($K_3[Fe(CN)_6]$), potassium ferrocyanide ($K_4[Fe(CN)_6]$), dimethylformamide (DMF), acetic acid, methanol, sodium acetate, and graphene powder were received from Sigma-Aldrich (München, Germany). 0.44 g of AMI powder was dissolved in distilled water to prepare a stock solution of AMI (10 mM), which was maintained at 4 °C. Graphene powder (1 mg) was dispersed in 1 ml of distilled water and ultrasonicated for 15 min to obtain the graphene oxide (GO) suspension. To prepare the supporting electrolyte, 5 M of $[Fe(CN)_6]^{3-/4-}$ was mixed with KCl (0.1 M). 0.1 M acetic acid and 0.1 M sodium acetate were used to prepare buffer solutions in the pH range of 2.0-7.0.

Instrumentation

Voltammetric experiments were performed using a digital potentiostat (Gamary, Interface 5000E/potentiostat/galvanostat/ZRA), a three-electrode cell consisting of a modified GCE (working electrode), platinum wire as the counter electrode, and a standard calomel electrode (reference electrode). Potentiometric measurements were made with a standard calomel electrode (SCE) as the reference electrode and modified GCE as the working electrode on a digital potentiometer. The surface morphologies of the synthesized polymers were investigated using a scanning electron microscope (SEM, JEOL JSM.6510LV, Japan) at 20 kV and magnification of 30000×. The 3D images were obtained via atomic force microscopy at a frequency setting of 0.1-100 Hz, measurement time less than 1 min, and maximum scanning (X, Y, Z) 5× 5 um × 1381 nm (AFM, Shimadzu, Wet-SPM9600, Japan). Furthermore, the composition of prepared polymers was studied using an FT-IR spectrometer in the range from 4000 cm^{-1} to 400 cm^{-1} (FT-IR, Thermo scientific, NICOLETiS10, USA).

Preparation of MIP

MIP for AMI was prepared by a thermal polymerization approach. Firstly, 0.5 mmol of AMI was dissolved in 20 ml distilled water and then mixed with 2 mmol MAA and 2 mmol AM. The mixture was stirred for 20 min to allow the functional monomers to interact with AMI molecules. Subsequently, EGDMA (10 mmol) and potassium persulfate (0.15 g) were added with continuous stirring until homogenization. The mixture was purged with N_2 gas for 10 min and heated at 60 °C in a water bath for 24 h to complete the polymerization process. Finally, the AMI molecules were extracted from the polymeric matrices using methanol/acetic acid (10%). For comparison, a non-imprinted polymer (NIP) was obtained using identical processes, but without the AMI template.

Electrochemical Sensors Fabrication

To prepare the voltammetric sensor, the surface of the GCE was cleaned with alumina slurry (0.05 μm) and then washed with methanol and distilled water. GO was synthesized using the Hummers method [31], and deposited on the GCE surface. Consequently, the MIP suspension was dropped onto the modified electrode (GO/GCE) and kept at room temperature to dry to perform an imprinted voltammetric sensor (MIP/GO/GCE). For comparison, a non-imprinted voltammetric electrochemical sensor (NIP/GO/GCE) was fabricated using the same protocol. The prepared working electrode was immersed in a buffered solution of AMI for cyclic voltammetry (CV) measurements. Electrochemical impedance spectroscopy (EIS) analysis was performed in a $[Fe(CN)_6]^{3-/4-}$ solution mixed with KCl (0.1 M). Moreover, under optimized conditions, the electrochemical determination of AMI was accomplished using differential pulse voltammetry (DPV). On the other hand, the selective potentiometric sensor (MIP/PVC/GCE) was constructed on the GCE surface. Briefly, PVC (0.5 g) was slowly dissolved in 20 ml DMF followed by the addition of MIP (0.03 g) and different plasticizers (DOP, TCP, DOS, o-NPOE, or DBP). After washing the GCE electrode surface as previously described, it was immersed in the mixture and dried in air.

Sample Preparation

Analytical applications of the proposed sensors were investigated using pharmaceutical tablets. The tablets were ground and diluted with an appropriate amount of distilled water. The solution was then buffered with acetate solution

at pH 4 and transferred into an electrochemical cell. Subsequently, the electrochemical signals (current (voltammetric technique) and/or potential (potentiometric technique)) were recorded, and the concentration of AMI was calculated based on the obtained calibration curves.

For urine samples, each sample was filtered, diluted with the appropriate buffer solution, and transferred to an electrochemical cell. Then, the AMI concentration was determined using both techniques. To assess the repeatability and reproducibility of these techniques, each urine sample was analyzed again after the standard addition of 5 and 10 μM AMI. Informed consent was obtained from all participants in the study and all procedures were approved by the institutional research board of Mansoura Faculty of Medicine, Mansoura University (MS.21.04.1442). All methods were performed in accordance with relevant guidelines and regulations.

RESULTS AND DISCUSSION

MIP Characterization

Morphology of the synthesized polymers. The surface morphologies of the synthesized polymers were investigated using SEM and AFM. As shown in Fig. 2, it was observed that the leached polymer had a relatively rough surface compared with the un-leached MIP, with uniformly distributed pores. The porosity and roughness of the imprinted polymer sharply elevated from 393.7 nm to 549 nm after leaching the AMI template.

IR and elemental analysis results. The chemical modification of the synthesized polymers was also identified using FT-IR spectroscopy (Fig. S1 (Supplementary Material)). As presented in the un-leached MIP spectrum, significant bands at wavenumbers of 3500, 1700, and 1250 cm^{-1} were assigned to COOH, C=O stretching, and bending, respectively. Moreover, the band at 1557 cm^{-1} in the un-leached MIP spectra belongs to pyrimidine (compared with the AMI spectrum) [32]. This band confirmed the successful insertion of AMI molecules into the polymer during polymerization. Furthermore, there are similarities between the IR spectra of leached MIP and NIP, which emphasize that their backbone structures are the same and ensure the complete removal of the AMI template during the extraction process. In addition, elemental analysis of leached MIP and un-leached MIP was performed and the results are listed in Table S1 (Supplementary Material). The high content of nitrogen in the un-leached MIP compared with the leached MIP revealed the presence of the AMI template in the polymeric matrix.

Potentiometric Sensor Response

The performance of potentiometric sensors was evaluated using the IUPAC guidelines. Briefly, MIP/PVC/GCE (working electrode) and saturated calomel (reference electrode, SCE) electrodes were attached to a pH/mv meter to measure the electromotive force (EMF). The EMF was calculated for different concentrations of AMI solutions to study the performance of the proposed sensor, and a calibration graph was constructed by plotting the potential reading versus the logarithmic concentration of AMI. As a control, a non-imprinted potentiometric sensor (NIP/PVC/GCE) without the AMI template was applied using the same techniques. As exhibited in Fig. 3, the leached imprinted potentiometric sensor showed a good response towards AMI molecules in the concentration range of 2.6×10^{-9} M to 3.1×10^{-3} M with a detection limit of 1.5×10^{-10} M. In contrast, the NIP/PVC/GCE sensor demonstrated a lower response to AMI than the MIP/PVC/GCE sensor. This behavior may be explained by the effect of the variation of AMI on the potential difference, which is generated in the electrochemical cell. The superb performance of the imprinted sensor over that of the non-imprinted sensor may be due to the presence of a selective ionophore (MIP), which forms a large number of particular active sites specified for AMI molecules. AMI molecules induced an inward flux toward the MIP/PVC/GCE. At higher AMI concentrations, a large number of active sites are occupied by AMI molecules through hydrogen bonds, resulting in high-potential signals. In contrast, the potentiometric signals dramatically diminished at low AMI concentrations, in which the imprinted sites were partially covered by AMI. After that, the stability of the potential values was exhibited, which demonstrates the complete coverage of the imprinted cavities.

Also, the reproducibility of the AMI solution was evaluated by a relative standard deviation (RSD) of 3.6% (n = 6). These results suggest excellent reproducibility and high stability of the developed sensor. Furthermore, the

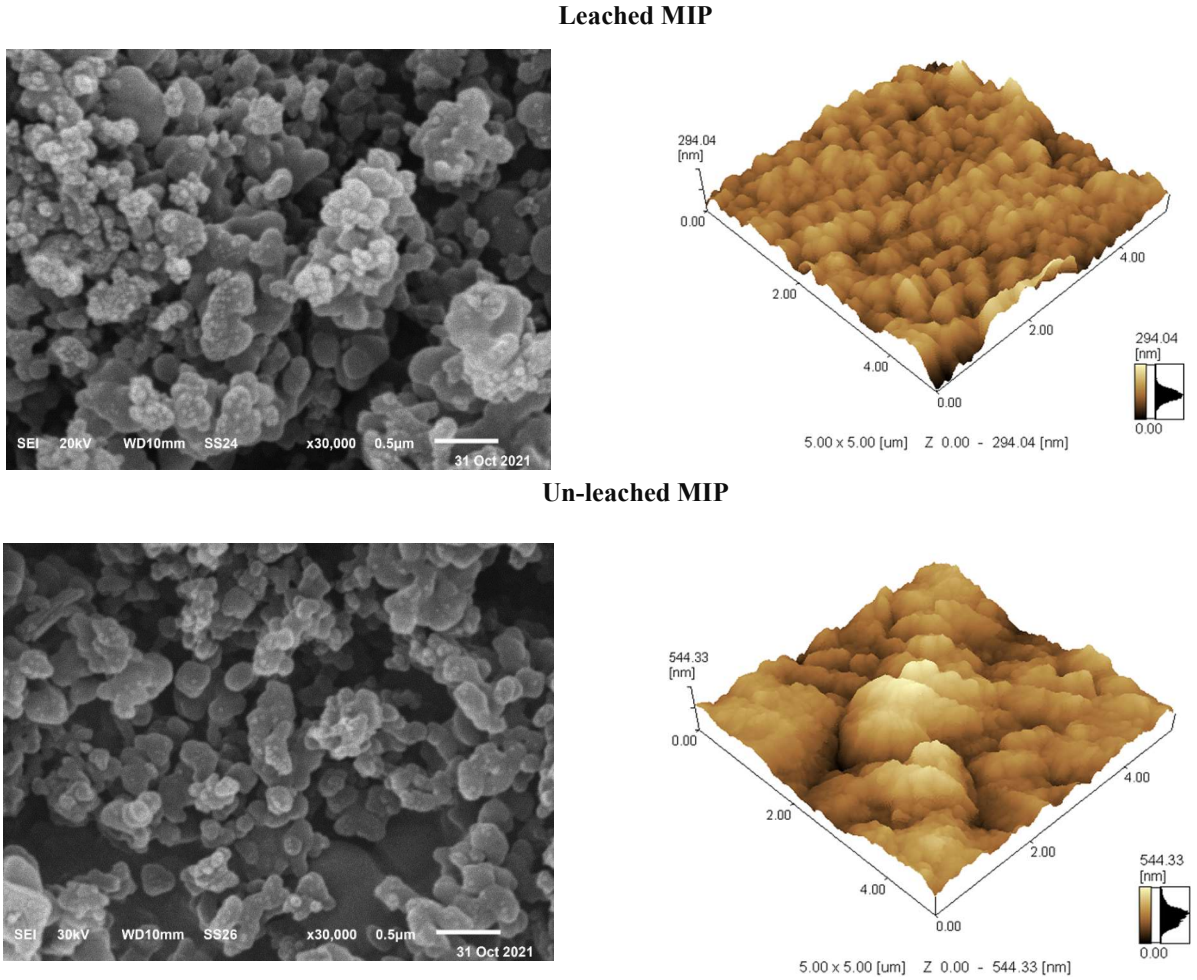

Fig. 2. SEM and AFM images of leached and un-leached imprinted polymers.

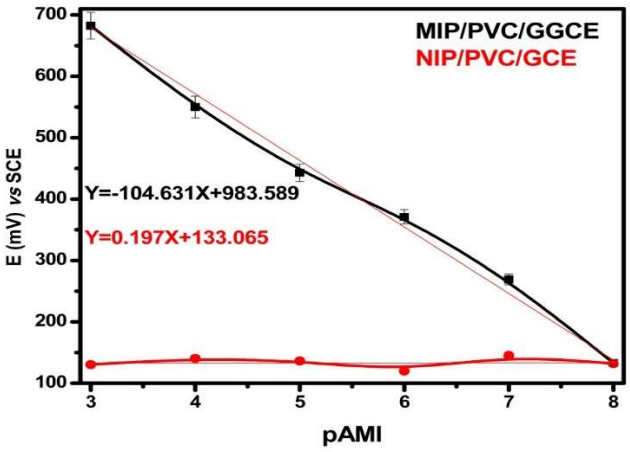

Fig. 3. The calibration plot of potentiometric sensors was recorded at pH 4.

potentiometric signals were acquired regularly for 2 months and compared to the primary results to assess the stability of the proposed sensor. After five weeks, there were no noticeable changes in the potentiometric signals.

Voltammetric Sensor

In electrochemical experiments, CV is commonly employed to detect analyte behavior. When comparing the voltammogram of buffered AMI solution to acetate buffer alone, a new significant signal at 0.9 V was noticed that indicated the AMI is electrochemically active. To further understand the electrochemical behavior of AMI on various surfaces of the prepared sensors, cyclic voltammograms were acquired at bare and modified electrodes in AMI solutions buffered with acetate at pH 4 (Fig. 4). Compared with the

bare GCE, the highest oxidation peak current was noticed for the GCE after modification with GO because of its large surface area, high conductivity, and faster electron transfer. Also, the addition of NIP or un-leached MIP to the GO/GCE surface resulted in a decrease in the peak values. This result indicates that the presence of these layers restricted the electrical conductivity of the surface. In contrast, the electrical response sharply increased when the GO/GCE was modified with leached MIP due to the formation of imprinted cavities on the electrode surface after the removal of AMI molecules. Electrochemical impedance spectroscopy is a useful technique for examining the surface characteristics of modified electrodes using the redox probe $[Fe(CN)_6]^{3-/4-}$. The impedance graphs of the bare and modified electrodes are shown in Fig. S2A (Supplementary Material). The charge transfer resistance (R_{ct}) was equal to the diagonal diameter of the plots, and the electron transfer capacity reduced as the R_{ct} value increased. As exhibited in the figure, the semicircle diameter decreased as a result of GO electrode modification. This observation confirms the high conductivity of GO. The R_{ct} value of MIP/GO/GCE was lower than that of the un-leached MIP/GO/GCE. These results emphasize the successful removal of the AMI templates and the formation of cavities that facilitate the passage of the redox probe to the electrode surface. Furthermore, the EIS has elaborated again in AMI (5×10^{-3} M) and KCl (0.1 M) to investigate the accessibility of AMI toward the modified GCE surface. As exhibited in Fig. S2B (Supplementary Material), high R_{ct} values were recorded for un-leached MIP/GO/GCE, while the R_{ct} sharply decreased after the removal of the AMI template due to the presence of different cavities at the surface of the polymer. Overall, the EIS results are consistent with the data obtained from the CV studies.

Parameters Optimization

Influence of pH. It is necessary to study the effect of pH on the performance of the electrochemical sensors. The effect of pH on the voltammetric and potentiometric sensors was studied in the pH range of (2-7). As shown in Fig. 5A, protonation of AMI may cause an apparent decrease in the voltammetric readings at lower hydrogen ion concentrations. Sharply elevation was observed with increasing pH values till reached the maximum current at pH 4 and then decreased slightly at higher pH values. These results may be attributed

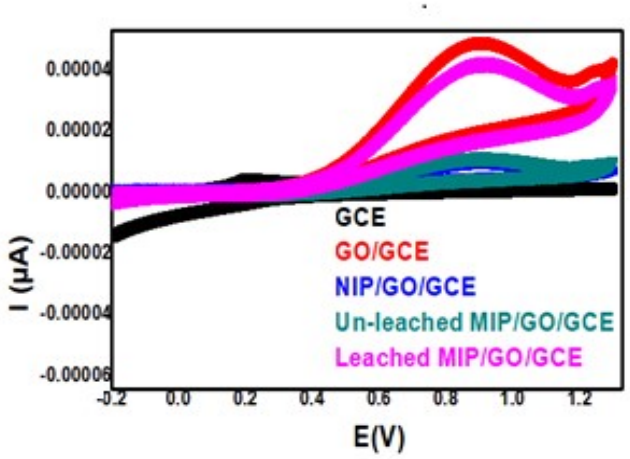

Fig. 4. Cyclic voltammograms for 5 mmol AMI and KCl (0.1 M) on bare GCE and different modified GCEs.

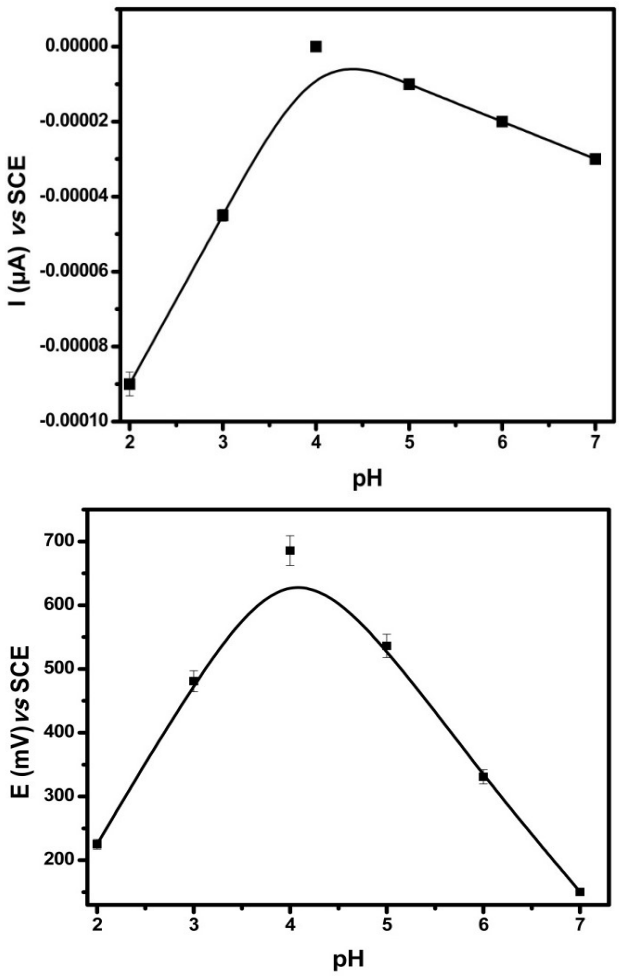

Fig. 5. Effect of pH on (A) voltammetric (B) potentiometric sensors.

to the competition between hydroxide ions and the AMI molecules at the electrode surface. Therefore, pH 4 was selected as the optimum pH for subsequent experiments. Moreover, for the MIP/PVC/GCE sensor, the electrode response gradually increased until pH reached 4 (Fig. 5B).

Influence of elution solvent and time. To renew the surface of the sensors, the AMI that occupies the imprinted cavities during measurements should be eluted. Methanol with different acetic acid ratios was used as the washing solution. Complete removal of AMI molecules was achieved using 10% (v/v) methanol-acetic acid. Furthermore, the elution time required for successful AMI template removal was investigated. As shown in Fig. S3 (Supplementary Material), 60 s and 90 s times were considered suitable removal times for voltammetric and potentiometric sensors, respectively, in which both electrodes regenerated their activity by removing the adsorbed AMI from the polymeric surfaces.

Selectivity of the sensors. To assess the selectivity of the voltammetric sensor for AMI, we checked the peak current in AMI solution when mixed with different competing molecules, including xanthine (Xa), caffeine (CF), theobromine (TH), paraxanthine (PA), and 1,3,7-trimethyl uric acid (TR). Nearly constant response values were noticed for the AMI in the presence of other interfering molecules. These results suggest a good selectivity for AMI owing to the presence of imprinted cavities that are complementary not just in shape but also in terms of functionalities. In addition, the calculated imprinted factor (the ratio of the peak current between the MIP sensor and NIP sensor) for AMI is (6.2). As a result, the sensing system exhibited excellent selectivity for AMI. Furthermore, the selectivity of the MIP/PVC/GCE sensor was evaluated using a fixed-interference method. This technique involves preparing several solutions with various AMI concentrations in the presence of a constant amount of comparable interfering molecules (I), and potentiometric signals are then measured. Subsequently, the selectivity coefficients ($K_{pot}^{AMI, I}$) were calculated using Eq. (1).

$$K_{pot}^{AMI,I} = a_{AMI}/(a_I)^{zAMI/zI} \quad (1)$$

where a, and Z are the activities and charges of AMI and the interfering molecules, respectively. As shown in Table S2 (Supplementary Material), there was no significant change in the performance of the potentiometric sensor in the presence of 100 to 150-fold excess of various interfering molecules due to the presence of specific stereochemical cavities on the polymeric surface which facilitates the attachment of the AMI only.

Influence of type of plasticizer and response time. The influence of the plasticizer type on the potential response was investigated. Different plasticizers, DOP, DOS, TCP, DBP, and o-NPOE (ε = 3.8, 5.2, 17.6, 5.0, and 24, respectively) were examined. It can be seen that the electrode with the DOP membrane has the highest response toward AMI compared to other plasticizers. In addition, the DOP membrane had a shorter response time (≤5 s), the average time required for each measurement to reach a stable reading, in the concentration range of 2.6×10^{-9} to 3.1×10^{-3} M with a ten-fold concentration difference (Fig. S4 (Supplementary Material)). The most appropriate explanation is that plasticizers, which have a high dielectric constant, have a reverse influence not only on the mobility of the synthesized polymer at the GCE surface but also on the net transfer of anionic species from the membrane phase to the aqueous phase.

Effect of the scan rate. A series of CV experiments with various scan rates ranging from 50 to 350 mV s^{-1} were carried out to investigate the effect of the scan rate on the current intensity. The current intensity gradually increased and varied linearly with the square root of the scan rate (Fig. S5a (Supplementary Material)), indicating that the electrochemical process is controlled by diffusion. In addition, Fig. S5b (Supplementary Material) shows a linear relationship between the peak potential and log υ, as expressed in Eq. (2). Furthermore, the Tafel equation was applied to calculate the number of electrons transferred during the redox reaction, which was equal to two (Fig. 6) [33,34].

$$E_{p,a}\,(mV) = 0.1 \log\upsilon + 0.05 \; (R^2 = 0.99) \quad (2)$$

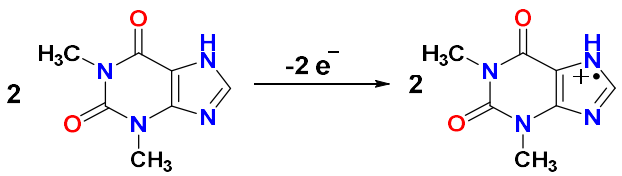

Fig. 6. The chemical oxidation of aminophylline.

Analytical Performance

The analytical performance of the proposed sensors for the determination of AMI was evaluated under optimum conditions. The voltammetric sensor had a linear response to AMI concentrations ranging from 3.7×10^{-11} M to 1×10^{-3} M with a detection limit of 2.1×10^{-12} M, based on measurements carried out by differential pulse voltammetry (DPV) (Fig. 7). In contrast, the response of the potentiometric sensor was directly proportional to the AMI concentration in the range of 2.6×10^{-9} M to 3.1×10^{-3} M. Analytical results, including the linear range, the limit of detection, stability, and reproducibility, are listed in Table S3 (Supplementary Material). Moreover, the data listed in Table 1 cover all the details of other techniques used for AMI detection. Overall, the developed sensors exhibited a better linear range, good sensitivity, and high stability.

Real Sample Analysis

Analytical applications of the proposed sensors were investigated using pharmaceutical and urine samples. Urine samples were collected from patients treated with AMI. Furthermore, to assess the repeatability and reproducibility of the operations, the standard addition of 5 mg l^{-1} and 10 mg l^{-1} of AMI in each urine sample was established. The concentration of AMI was measured in these sample solutions according to the developed methods. As shown in Table S4 (Supplementary Material), good recoveries ranging from 98.2% to 99.6% were observed for the detection of AMI, with an RSD of less than 2.4%. These results indicate that the proposed sensors have high accuracy and can be applied to AMI drug and urine sample monitoring.

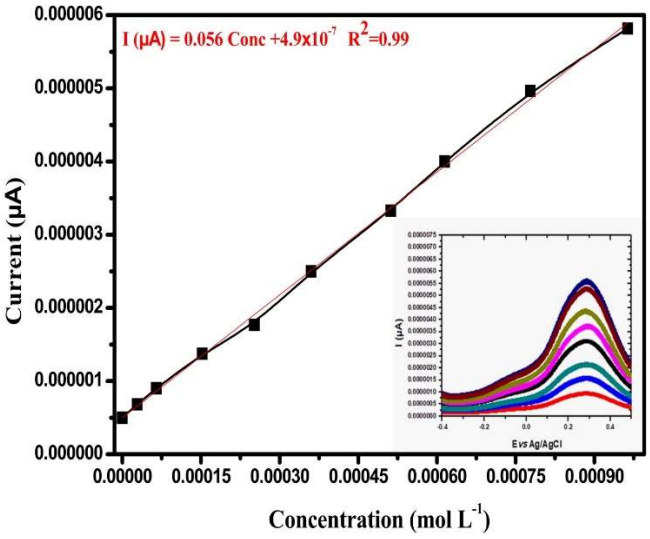

Fig. 7. DPV of MIP/GO/GCE after incubation in various concentrations of AMI (pH = 4, scan rate = 100 mv s^{-1}, pulse amplitude = 25 ms).

CONCLUSION

In the present study, new MIPs were fabricated and employed for the electrochemical sensing of AMI in real samples. The prepared polymers were characterized by using FT-IR, SEM, and AFM. The MIP with GO was used to modify the surface of the GCE to perform the voltammetric sensor. A potentiometric sensor was fabricated using polyvinyl chloride and the synthesized polymer. According to the results, the voltammetric sensor had a lower detection limit of 2.1×10^{-12} M and a dynamic response range of 3.7×10^{-11} M to 1×10^{-3} M, whereas the potentiometric sensor had a concentration range was (2.6×10^{-9}-3.1×10^{-3} M) with a detection limit of 1.5×10^{-10} M. In addition, the proposed methods showed high selectivity and good reproducibility and were successfully applied for AMI detection in pharmaceutical drugs and urine samples with recovery values (98.2-99.6%).

REFERENCES

[1] S. Sundaran, Buvaneswari, S. Muralidharan, M. Saji, S. D. Rajendran, S. Sankar, Asian J. Pharm. Clin. Res. 6 (2013) 30.

[2] V.Y. Chock, S. Cho, A. Frymoyer, Pediatr. Res. 89 (2021) 974.

[3] A. Peng, Y. Wang, J. Xiao, S. Wang, H. Ding, Anal. Methods 8 (2016) 1069.

[4] G.C. Wall, H.L. Smith, M.W. Trump, J.D. Mohr, S.P. DuMontier, B.L. Sabates, L. Ganapathiraju, T.J. Kable, Clin Respir J. 15 (2021) 843.

[5] J.M. Khalaf, I.I. Hussein, M.S. Al-Nimer, J. Res. Pharm. 25 (2021) 852.

[6] C. Ye, C. Miao, L. Yu, Z. Dong, J. Zhang, Y. Mao, X. Lu, Q. Lyu, Pediatr. Neonatol. 60 (2019) 43.

[7] B. Yin, J. Li, S.-l. Wang, S. Yan, C. Sui, S. Wan, F.

Liu, R. Wan, Eur. J. Drug Metab. Pharmacokinet. 41 (2016) 19.

[8] A.R.S. Babu, B. Thippeswamy, A.B. Vinod, E. G. Ramakishore, S. Anand, D. Senthil, Pharm. Methods. 2 (2011) 211.

[9] J. Ge, F. Tong, Y. Li, Y. Zhang, Q. Chu, J. Ye, Chinese J. Chem. 31 (2013) 525.

[10] S. Mazurek, R. Szostak, J. Pharm. Biomed. Anal. 40 (2006) 1235.

[11] Q. Li, H. Zhang, Spectrochim. Acta Part A Mol. Biomol. Spectrosc. 70 (2008) 284.

[12] R.Y. Wang, J. Wu, L.J. Wang, R. Wang, H. Dou, Opt Spectrosc (English Transl Opt i Spektrosk. 115 (2013) 596.

[13] B. Rezaei, A.A. Ensafi, L. Zarei, Spectrochim Acta- Part A Mol. Biomol. Spectrosc. 90 (2012) 223.

[14] M.E. Khalifa, T.A. Ali, A.B. Abdallah, Anal. Sci. 37 (2021) 955.

[15] A.B. Abdallah, A. Saher, A.F.S. Molouk, W.I. Mortada, M.E. Khalifa, Biosens. Bioelectron. 208 (2022) 114213.

[16] A.B. Abdallah, M.R. El-kholany, A.F.S. Molouk, T.A. Ali, A.A. El-Shafei, M.E. Khalifa, RSC Adv. 11 (2021) 30771.

[17] Ç. Öter, Ö.S. Zorer, Chem. Eng. J. Adv. 7 (2021) 1.

[18] T. Cai, Y. Zhou, H. Liu, J. Li , X. Wang, S. Zhao, B. Gong, J. Chromatogr. A 1642 (2021) 462009.

[19] S. Yang, Y. Zheng, X. Zhang, S. Ding, L. Li, W. Zha, J. Solid State Electrochem. 20 (2016) 2037.

[20] X. Liu, J. Zhong, H. Rao, Z. Lu, H. Ge, B. Chen, P. Zou, X. Wang, H. He, X. Zeng, Y. Wang, J. Solid State Electrochem. 21 (2017) 3071.

[21] T. Gan, A. Zhao, Z. Wang, P. Liu, J. Sun, Y. Liu, J. Solid State Electrochem. 21 (2017) 3683.

[22] M. Shamsipur, N. Moradi, A. Pashabadi, J. Solid State Electrochem. 22 (2018) 169.

[23] A.B. Abdallah, E.A. Ghaith, W.I. Mortada, A.F.S. Molouk, Food Chem. 401 (2023) 134058.

[24] M. Singh, S. Singh, S.P. Singh, S.S. Patel, Trends Environ. Anal. Chem. 27 (2020).

[25] S. He, L. Zhang, S. Bai, H. Yang, Z. Cui, X. Zhang, Y. Li, Eur. Polym. J. 143 (2021) 110179.

[26] M.A. Tabrizi, J.P. Fernández-Blázquez, D.M. Medina, P. Acedo, Biosens. Bioelectron. 196 (2022) 113729.

[27] Y. Saylan, S. Akgönüllü, H. Yavuz, S. Ünal, A. Denizli, Sensors 19 (2019) 1279.

[28] W. Song, Y. Chen, J. Xu, X. Yang, D. Tian, J. Solid State Electrochem. 14 (2010) 1909.

[29] Y. Hu, Z. Zhang, H. Zhang, L. Luo, S. Yao, J. Solid State Electrochem. 16 (2012) 857.

[30] X. Kan, T. Liu, C. Li, H. Zhou, Z. Xing, A. Zhu, J. Solid State Electrochem. 16 (2012) 3207.

[31] J. Chen, B. Yao, C. Li, G. Shi, Carbon. 64 (2013) 225.

[32] S. Breda, I.D. Reva, L. Lapinski, M.J. Nowak, R. Fausto, J. Mol. Struct. 786 (2006) 193.

[33] Y. Wang, L. Wang, H. Chen, X. Hu, S. Ma, ACS Appl. Mater. Interfaces. 8 (2016) 18173.

[34] L. Wang, C. Wang, Microchim. Acta 153 (2006) 95.

[35] F. Chen, B. Fang, S. Wang, J. Anal. Methods Chem. 2021 (2021) 1.

[36] C. Feng, H. Wu, S. Lin, S. Chen, J. Liq. Chromatogr. Relat. Technol. 26 (2003) 1913.

[37] Q. Li, H. Zhang, Spectrochim. Acta Part A. Mol. Biomol. Spectrosc. 70 (2008) 284.

[38] Q. Li, T. Zhang, W. Lv, Eur. J. Med. Chem. 44 (2009) 1452.

[39] M. Wang, B. Tian, Y. Xue, R. Li, T. Zhai, L. Tan, Spectrochim. Acta Part A Mol. Biomol. Spectrosc. 235 (2020) 118306.

[40] A. Câmpean, M. Tertiș, R. Săndulescu, Cent. Eur. J. Chem. 9 (2011) 688.